Brazilian Journal
of Chemical
Engineering

ISSN 0104-6632
Printed in Brazil
www.abeq.org.br/bjche

Vol. 33, No. 04, pp. 957 - 967, October - December, 2016
dx.doi.org/10.1590/0104-6632.20160334s20150333

SYNTHESIS OF CUMENE BY TRANSALKYLATION OVER MODIFIED BETA ZEOLITE: A KINETIC STUDY

R. Thakur, S. Barman* and R. Kumar Gupta

Department of Chemical Engineering, Thapar University, Patiala-147004, Punjab, India.
Phone: + 91-175-2393437; Fax: + 91-175-239300
E-mail: sbarman@thapar.edu

(Submitted: May 26, 2015 ; Revised: September 25, 2015 ; Accepted: October 29, 2015)

Abstract - In the present study, transalkylation of 1,4-diispropylbenzene (DIPB) with benzene in the presence of modified beta zeolite was performed to produce cumene in a fixed bed reactor. Beta zeolite was exchanged with cerium in order to modify its catalytic activity. Activity of the modified catalyst was evaluated in the range of temperature 493K–593K, space time 4.2 kg h/kmol–9.03 kg h/k mol and benzene/1,4-DIPB molar ratio 1–15 to maximize the reactant conversion and selectivity of cumene. The activity and selectivity of the modified catalyst was found to increase with increase in cerium loading. Maximum selectivity of cumene (83.82%) was achieved at 573 K, benzene/1,4-DIPB 5:1 at one atmosphere pressure. A suitable kinetic model for this reaction was proposed from the product distribution pattern following the Langmuir–Hinshelwood approach. Applying non-linear regression, the model parameters were estimated. The activation energy for the transalkylation reaction was found to be 116.53 kJ/mol.
Keywords: Cerium; Beta zeolite; Kinetic study; Transalkylation; DIPB; Benzene.

INTRODUCTION

Cumene is a colorless liquid, also known as cumol or isopropyl benzene having the boiling-range motor fuel of high antiknock value. It is of industrial demand for the production of high molecular weight hydrocarbons such as cymene and polyalkylated benzene. The main end uses for cumene are for the production of phenolic resins, bisphenol A, and caprolactam. However, 5-10 wt% diisopropylbenzene (DIPB) isomers are produced as low value byproduct during the isopropylation of benzene to cumene (Leu *et al*., 1990; Sridevi *et al*., 2001; Reddy *et al*., 1993). The by-products, DIPB isomers, can be recycled for cumene production, making this process more economical. With the liquid catalysts, there are inherent problems of product separation, recycling and corrosiveness (Maity and Pradhan, 2006; Barman *et al*., 2005; Ercan *et al*., 1998). In that respect, zeolites can exhibit acidities close to those of traditional mineral acid solutions and hence proved to be better catalyst (Best and Wojciechowski, 1978; Slaugh, 1983; Bakas and Barger, 1989). Moreover, the number and strength of acid sites in zeolite can be changed to a great extent by exchanging its H^+/Na^+ ions with rare earth cations in the zeolite framework. A comparative study was carried out on transalkylation of DIPB with benzene over Y, beta and mordenite with different Si/Al molar ratios in supercritical CO_2 and liquid phase (Sotelo *et al*., 2006). The influence of Si/Al ratio on the activity of catalyst was explained in terms of cumene selectivity and yield considering the competitive isomerization and by-product formation. The use of supercritical CO_2 did not show superior catalytic transalkylation activity for the Y zeolite. In Mobil Oil Corp., USA, production of cumene was carried

*To whom correspondence should be addressed

out by introducing the feed to a transalkylating zone over beta zeolite/alumina and then feeding to an alkylating zone where MCM-22/alumina catalyst was used (Collins *et al*., 1999). Transalkylation of DIPB has also been carried out over large pore zeolites, which proved to be very active catalysts (Pradhan and Rao, 1993). In another process, DIPBs were recycled for transalkylation in the reactor containing a single catalyst bed of beta catalyst. The combined alkylation and transalkylation was performed for alkyl aromatic production to evaluate the performance of different catalysts like MCM-22 and beta zeolite based on their Si/Al ratio, selectivity, and pore size for liquid phase production of cumene (Perego and Ingallina, 2004). The catalysts such as zeolite X, MCM-22, MCM-49, PSH-3, SSZ-25, zeolite Y, beta zeolite (Yeh *et al*., 2008; Barger *et al*., 1989; Huang *et al*., 1997) were used in transalkylation reaction. These studies show that choice of catalyst, its Si/Al ratio and the acidity of the catalyst highly affect the process.

Kinetics of transalkylation of diisopropylbenzene were studied over Ca modified YH zeolite catalyst which proved to be a good active catalyst (Grigore *et al*., 2001). Cumene synthesis over beta zeolite has been reported in the literature (Bellussi *et al*., 1995; Perego *et al*., 1996; Smirnov *et al*., 1997; Halgeri and Das, 1999). Therefore, further investigation was necessary to carry out transalkylation of DIPB with benzene over the modified beta zeolite to obtain higher cumene selectivity and reactant conversion. Replacement of sodium ions in zeolites with polyvalent cations like rare earth metals (La, Ce, etc.) has been reported to produce materials of superior catalytic activity (Venuto *et al*., 1966; Rabo *et al*., 1968; Hunter and Scherzer, 1971). However, very scarce literature is available on the use of rare earth metal modified beta zeolite for cumene synthesis. It was, therefore, thought desirable to investigate the kinetics of this commercially important reaction over zeolite H-beta modified by exchanging H^+ ions with cerium ions. A further objective of this study was to develop a suitable kinetic model for the synthesis reactions.

MATERIALS AND METHODS

Materials

Beta zeolite, 1.5 mm extrudates, used in the present study, was obtained from Sud chemie, Vadodra, India. Ceric ammonium nitrate (99% pure) was procured from CDH chemicals, India. Benzene and 1,4-DIPB of analytical reagent grade ((>99% pure) were obtained from Sigma Aldrich Pvt. Ltd., India. Nitrogen gas (grade –I, 99.999% pure) was obtained from Sigma gases and services (India).

Catalyst Preparation

The commercially available H-beta zeolite containing H^+ ions was modified with Ce^{4+} ions. At first, the zeolite extrudates were calcined for 3 h at 623 K. Calcined zeolite was then refluxed with the required percentage of ceric ammonium nitrate solution at 363 K for 24 h, thereby modifying H-beta zeolite into the Ce-beta form. The catalyst particles were then filtered and washed several times with deionized water and then dried at 393 K for 14 h. Finally, they were calcined for 4 h at 723 K to remove the excess ions. The cerium-exchanged zeolite was characterized by TPD, XRD and FTIR. Beta zeolite treated with 4%, 6%, 8%, and 10% cerium ammonium nitrate solution (CeB_4, CeB_6, CeB_8, and CeB_{10}) was used for the present study.

Determination of Cerium in the Exchanged Catalysts

The amount of cerium ions exchanged with the H^+ ions was calculated analytically (Krishnan *et al*., 2002). Freshly calcined cerium modified beta zeolite was taken in a flask and digested for 1 h in concentrated HCl. The digested catalyst was diluted with distilled water and filtered. The filtrate was transferred to a beaker and its volume was made up to about 250 ml by adding distilled water. 50 ml of saturated oxalic acid solution was mixed with this solution, which produced a white precipitate of cerium oxalate. The precipitate was then filtered using a Whatman no.40 ashless filter paper and washed with distilled water. The filter paper was ignited in a previously weighed silica crucible at 1173±10 K to a constant weight. On heating, cerium oxalate was converted to cerium oxide. From the weight of cerium oxide the percentage of cerium was then calculated. CeB_4, CeB_6, CeB_8 and CeB_{10} were found to have been loaded with 2.87%, 4.46 wt%, 6.64 wt% and 8.34 wt% of cerium respectively.

Experimental Setup for Transalkylation Reactions

Vapor phase transalkylation reaction was carried out in a fixed-bed, continuous down-flow, stainless steel (SS 316) reactor. The reaction conditions were maintained at atmospheric pressure. A preheater was fitted with the reactor in the upstream and a condenser

in the downstream. A thermowell extending from the top of the reactor to the centre of the bed was used to measure the temperature of the reactor. Typically, 0.002 kg of the catalyst supported on a wire mesh was loaded into the reactor. Before conducting the experiments, catalyst activation was done at a temperature 100 K higher than the reaction temperature (maintained according to reaction conditions), for 3 h under the atmosphere of nitrogen. A dosing pump was used to introduce the reactant feed mixture into the reactor. Nitrogen gas was flown through the reactor at the rate of 0.565 L/h to activate the catalyst before experimental runs. However during all experimental runs, the nitrogen to feed flow rate ratio was kept constant at 0.2. The reactants were vaporized in the preheater, which is maintained at a temperature 30 K lower than the reaction temperature. The vaporised reactant feed mixture passes through the catalyst bed in the reactor at proper reaction conditions. The product vapors, along with the unreacted reactants, were condensed in the condenser (277 K-279 K). The samples were collected and analyzed in a gas chromatograph (Bruker, Model: 436 GC Scion) using a fused silica capillary column having 10 m × 0.53 mm × 1.5 μm dimensions. The sample was introduced through a micro syringe into the injector port of the GC. The temperature of the injector was set at 493 K during the analyses. The column temperature was initially set at 323K, and then increased to 523 K at a rate of 10 K/min. The flow rate of carrier gas (nitrogen) was maintained at 1.5 L/h. A Flame Ionisation Detector was used at 553 K to detect the products. Peaks were identified by retention time matching with known standards. Various products like aliphatics (propene), benzene, toluene, xylene (C_8), cumene, cymene (C_{10}), isomers of DIPB were found. The selectivity of cumene, 1,3 DIPB and conversion of 1,4 DIPB were calculated as:

$$1,4\ \text{DIPB conversion} = \frac{(1,4\ \text{DIPB in feed} - 1,4\ \text{DIPB in exit})}{(1,4\ \text{DIPB in feed})} \times 100$$

$$\text{Cumene selectivity} = \frac{(\text{Cumene in product mixture})}{(\text{aromatics in product excluding}\, 1,4\ \text{DIPB and benzene})} \times 100$$

$$1,3\ \text{DIPB selectivity} = \frac{(1,3\ \text{DIPB in product mixture})}{(\text{aromatics in product excluding}\ 1,4\ \text{DIPB and benzene})} \times 100$$

The mechanism of transalkylation of 1,4 DIPB with benzene is shown in Figure 1.

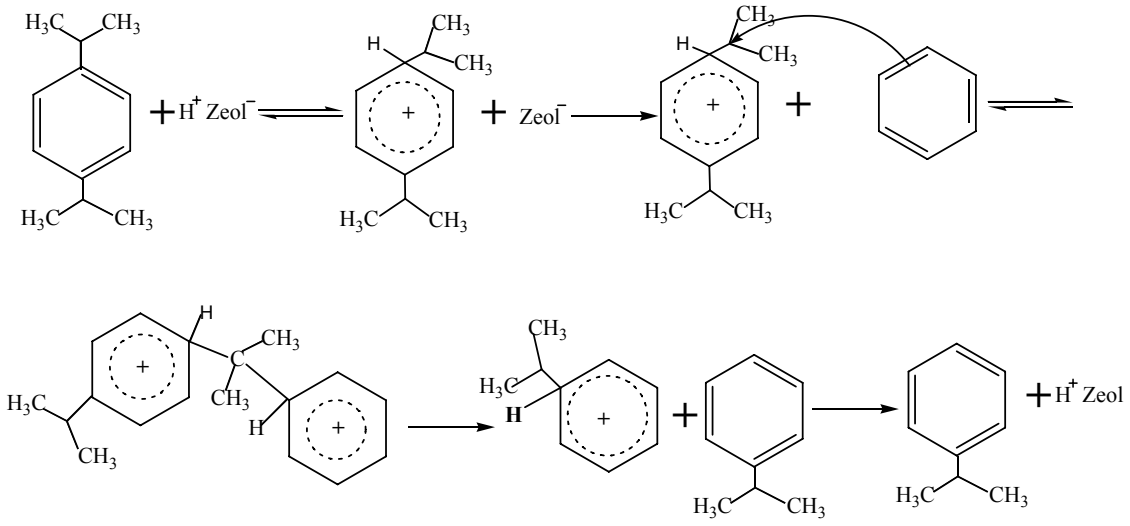

Figure 1: Mechanism of transalkylation of 1,4-DIPB with benzene.

RESULTS AND DISCUSSION

Characterization of the Modified Catalyst

The powder X-ray diffraction patterns of the zeolite samples were recorded on a Bruker Angle X-Ray Scattering Diffractometer D8, Germany with 2θ value in the range of 5^0-60^0 at a scanning speed of 2^0 (2θ) per minute. The diffractometer was equipped with a Ni-filtered Cu K-α radiation source. Sample preparation for the X-ray analysis involved gentle grinding of the solid into a fine powder. Approximately 0.1-0.2 g of the sample was taken into the sample holder with light compression to make it flat and tight. Ammonia Temperature Program Desorption of the parent and modified catalysts were performed in a CHEM-BET 3000 instrument (Quantachrome). Catalyst sample (0.1 g) was first degassed at 723 K for 1 h with nitrogen followed by cooling to 273 K temperature. Nitrogen-ammonia gas (1 mol%) mixture, was then passed through the sample for 1 h. The catalyst sample was heated to 372 K until the steady state was attained; thereafter the temperature of the sample was raised up to 1173 K at a heating rate of 10 K/min. The desorbed ammonia was detected by a Thermal Conductivity Detector analyzer. Studies of FTIR were done using an Agilant Cary-660 spectrophotometer in the range 400 cm^{-1}-4000 cm^{-1}. Samples were analysed by preparing KBr pellets. Sample was first ground thoroughly and then it was mixed with KBr salt and again ground well to make a fine powder, which was then pressed to make a pellet. It was then placed in the FTIR sample holder and 32 scans were taken for each sample.

Both modified and unmodified beta zeolites were characterized by XRD and are shown in the Fig. 2. Typical diffraction characteristics of BEA topology are observed for both the zeolites indicating the framework structure is well preserved after cerium exchange. The CeB_{10} diffractograms exhibited a high intensity reflection at $2\theta = 7.8^0$ and 21^0-22^0 which is a typical characteristic peak of beta zeolite (Zhang *et al*., 2014). This phenomenon indicates that the crystal structure of beta zeolite was not changed by metal exchange. The crystallinity of the modified sample was measured from the intensity of the peaks. At low loading of metal ions into the zeolite framework, no diffraction lines corresponding to metal species were observed as at low loading, the cerium ions replace the H^+ ions (Tang *et al*., 2014) and are highly dispersed in the zeolite framework (Garcia *et al*., 2011). However, on increasing the metal loading, additional peaks of metal oxides present on the catalyst surface appear in the XRD pattern (Siregar and Amin, 2006, Amin and Anggoro, 2003; Garcia *et al*., 2011). At high loading of cerium (10 wt%), additional peaks related to cerium oxide ($2\theta = 13.56^0$ and 46.5^0) were found in zeolite XRD pattern (Thakur *et al*., 2015). Similar observation was reported for high loading of cerium (16 wt%) into the beta zeolite framework (Wang and Zou, 2003).

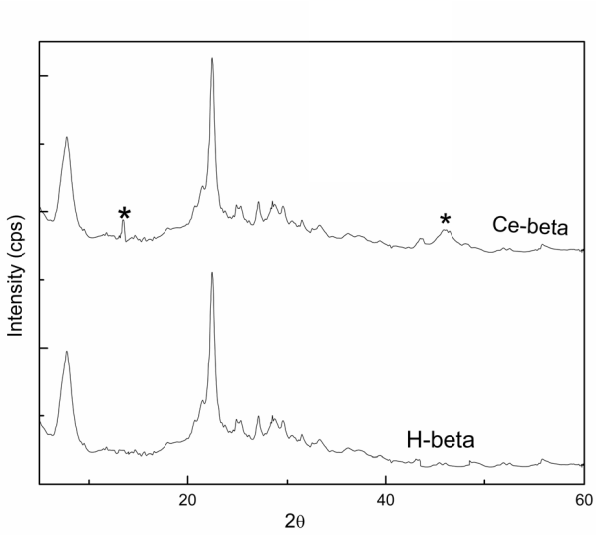

Figure 2: XRD of beta and cerium modified beta zeolite.

The temperature programmed desorption profile of ammonia was studied with H-beta and CeB_{10} beta zeolites and is shown in Fig. 3. The profiles show that the catalysts contain mainly two types of acid sites of different strengths. The low temperature peak is due to ammonia desorption from the weak acid sites, whereas, the peak at high temperature is due to the desorption of strongly adsorbed ammonia from strong acid sites. TPD profiles show that, in the case of H-beta zeolite, only weak acid sites are present. In the case of Ce-beta zeolite there is an additional peak in the higher temperature range (400-600 ºC) due to the presence of strong acid sites created by ion exchange. The strength of the acid sites increases with cerium content as the desorption peaks shift gradually towards the higher temperatures with increasing cerium in the catalysts (Barman *et al*., 2005). Moreover, the number of acid sites also increases as the peak area increases with Ce exchange. Thus, it can be concluded from Fig. 3 that cerium exchange leads to an increase in both quantity and strength of the acid sites in zeolite (Thakur *et al*., 2014; Wang and Zou, 2003). The acidity of H–beta zeolite was found to be 0.88 mmol/gm and that of cerium beta zeolite was 1.79 mmol/gm.

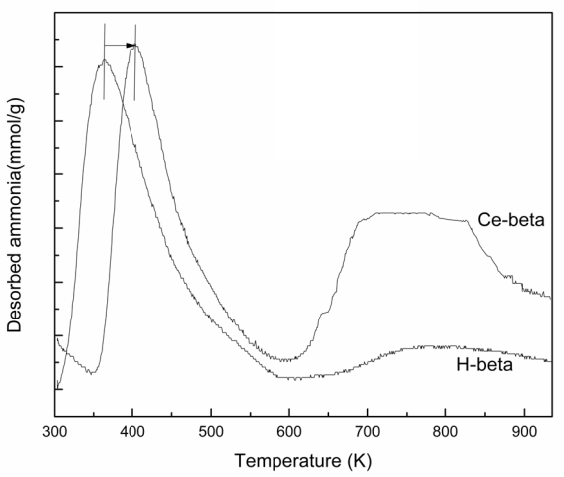

Figure 3: Ammonia-TPD profile of different beta zeolites.

The FTIR spectra of H-beta and cerium exchanged beta zeolite are shown in Fig. 4. The IR spectra of H-beta and CeB_{10} zeolite show major bands in the 450–1650 cm^{-1} region with additional bands at the 3450 cm^{-1} region. Beta zeolite shows bands approximately at 460, 520, 785, 1060, 1212, 1625 and 3440 cm^{-1}. The peak at 520 cm^{-1} is characteristic of beta zeolite (Kiri *et al*., 1994). The major characteristic bands at 460, 785, 1060 and 1212 cm^{-1} are attributed to a T-O bending mode, O-T-O external symmetric stretch and O-T-O internal asymmetric stretching vibrations and O-T-O external asymmetric stretch, respectively. In case of cerium-modified beta zeolite all the peaks show a little shift in peak positions. The additional absorption band at wavenumber 553 cm^{-1} represents the Ce-O stretch (Ansari *et al*., 2009). The intensities of peaks for the modified zeolite are greatly enhanced. The broad bands observed in the case of both catalysts at 3453 cm^{-1} are due to the stretching vibrations of hydroxyl groups, and those at 1635 cm^{-1} are lattice water molecules, respectively. This suggests that the zeolite framework remains unaffected after the ion exchange process and cerium exchange of beta zeolite.

Activity of Catalyst in the Transalkylation Reaction

The activity of Ce-beta zeolites and the parent H-beta zeolite were tested for a 3.5 h time period on stream at 573 K and atmospheric pressure. Fig. 5 shows that a maximum of 83.82% selectivity of cumene was obtained over CeB_{10}, which decreases to a value of 81.09% after 3.5 h on stream. This may be due to deactivation of zeolite by formation of coke, which blocks the catalyst surface. It is observed that the selectivity of cumene decreases with a decrease in cerium content of zeolite and was found to be 81.33% and 77.87% over CeB_8 and CeB_6 zeolites, respectively. Selectivity of cumene becomes lowest (73.23%) in the case of unmodified beta zeolite.

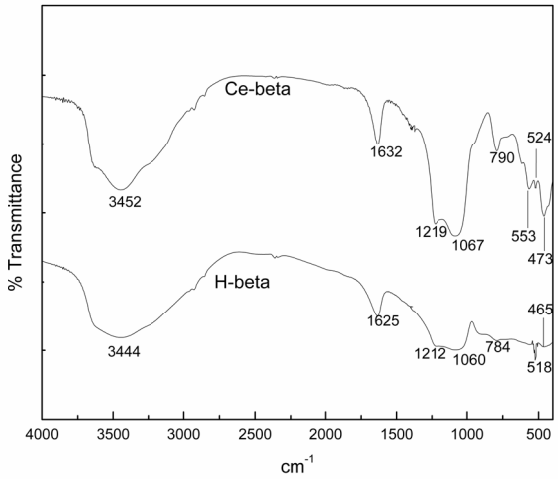

Figure 4: FTIR of H-beta and Cerium modified beta zeolites.

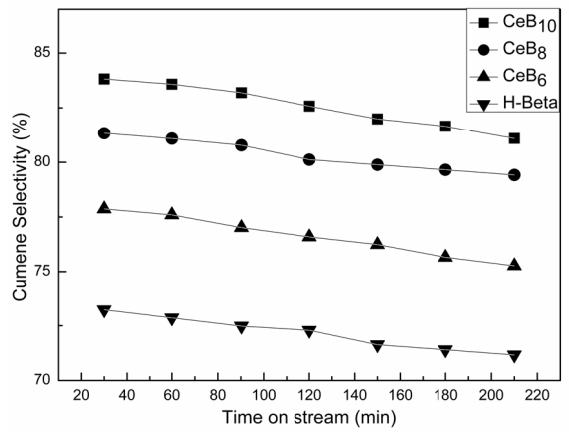

Figure 5: Cumene selectivity as a function of time-on-stream. Reaction Conditions: Pressure =1 atm, temperature = 573 K, benzene/1,4-DIPB = 5:1, space time = 9.03 kg h/ kmol, N_2 to feed ratio = 0.2, catalyst amount = 0.002 kg.

Effect of Temperature on DIPB Conversion and Product Selectivity

The effect of temperature on product selectivity is shown in Fig. 6 in the temperature range of 493 K-593 K over CeB_{10} catalyst. With the increase in temperature, the cumene selectivity increases gradually and reaches a maximum (83.82%) at 573 K but above this temperature the cumene selectivity is decreased due to the formation of the side product xylene.

The product distribution at different reaction temperatures is shown in Table 1. The conversion of DIPB was maximum (94.69%) at a temperature of 573 K and then decreased to 85.12% at 613 K. At

higher temperature the decrease in conversion is due to deactivation of the catalyst by deposition of coke on the catalyst surface.

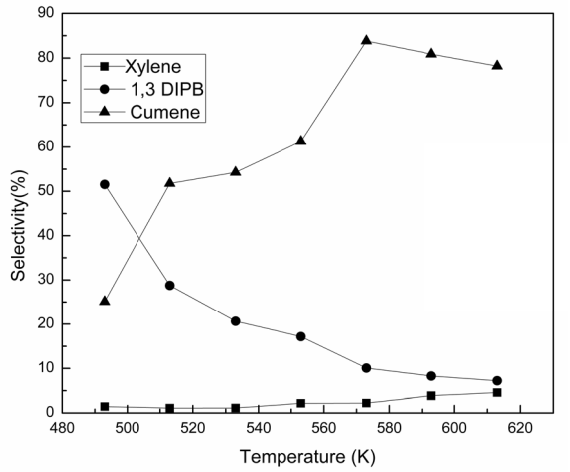

Figure 6: Effect of temperature on product selectivity (Reaction Conditions: Pressure =1 atm, benzene/ 1,4-DIPB ratio = 5:1, space time = 9.03 kg h/ k mol, N_2 to feed ratio = 0.2, time on stream = 30 min, catalyst (CeB_{10}) amount = 0.002 kg).

Table 1: Product distribution at different temperatures.

Product distribution (wt%)	Temperature (K)					
	493	513	533	553	573	593
Aliphatics	0.76	0.79	0.72	0.40	0.07	0.03
Benzene	67.15	67.07	66.91	63.27	47.21	56.40
Toluene	0.12	0.20	0.22	0.30	0.35	0.69
Xylene	0.17	0.23	0.31	0.74	1.14	1.55
Cumene	2.96	10.60	15.03	20.18	42.94	32.54
n-PB	0.29	0.35	0.41	0.50	0.58	1.56
C10	1.39	2.41	5.31	5.16	0.97	0.53
1,3-DIPB	6.10	5.89	5.72	5.66	5.17	3.33
1,4-DIPB	21.06	12.46	5.40	3.79	1.57	3.37
Cumene yield (%)	2.96	10.60	15.03	20.18	42.94	32.54
1,4-DIPB conv(wt%)	29.01	51.69	81.78	87.20	94.69	88.63

Reaction Conditions: Pressure =1 atm, benzene/1,4-DIPB ratio = 5:1, space time = 9.03 kg h/ kmol, N_2 to feed ratio = 0.2, time on stream = 30 min, catalyst (CeB_{10}) amount =0.002 kg.

Effect of Benzene to 1,4-DIPB Mole Ratio on Product Selectivity

In the transalkylation reaction, the benzene to 1,4 DIPB ratio was varied from 1 to 15 at a reaction temperature of 573 K and space time of 9.03 kg h/k mol. Fig. 7 shows that the maximum selectivity (83.82%) of cumene was obtained at a benzene to 1,4-DIPB ratio of 5:1, beyond this ratio, the isomerisation of 1,4-DIPB seems to increase and hence a decrease in cumene selectivity was observed.

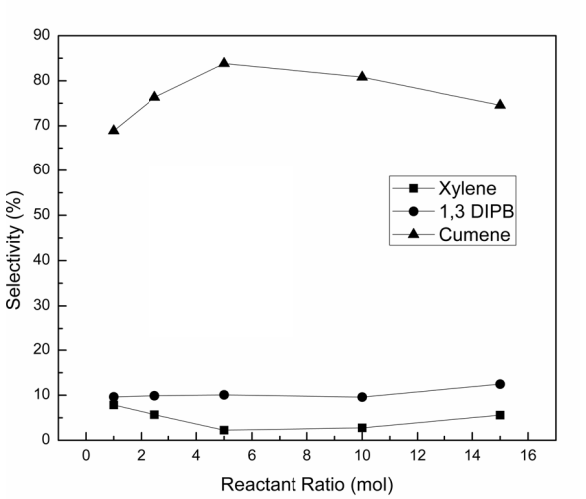

Figure 7: Effect of reactant mole ratio on product selectivity (Reaction Conditions: Pressure =1 atm, temperature = 573 K, space time = 9.03 kg h/ kmol, N_2 to feed ratio = 0.2, time on stream = 30 min, catalyst (CeB_{10}) amount = 0.002 kg).

Effect of Space Time on Selectivity of Products and Conversion of 1,4 DIPB

The effect of space-time was studied in the range of 4.21 kg h/k mol–9.03 kg h/k mol. The cumene selectivity increased with increase in space time and reached its maximum of 83.82% at a space time of 9.03 kg h/kmol. Higher contact time allows the reactants to remain in the vicinity of each other and the catalyst surface for longer time, therefore enhancing the transalkylation reaction instead of isomerisation and disproportionation. Selectivity of products as a function of space time is shown in Figure 8.

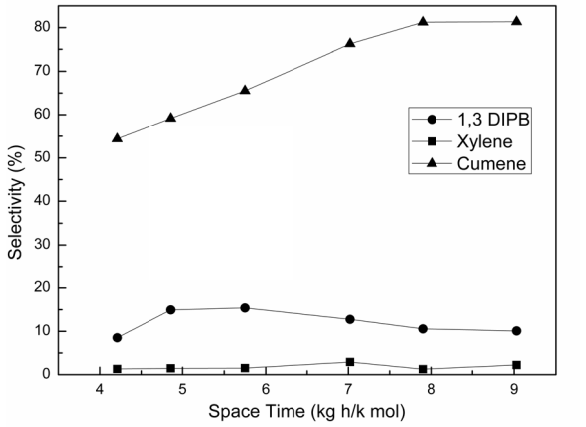

Figure 8: Effect of space time on product selectivity (Reaction Conditions: Pressure =1 atm, temperature = 573 K, benzene/1,4-DIPB ratio = 5:1, N_2 to feed ratio = 0.2, time on stream = 30 min, catalyst (CeB_{10}) amount = 0.002 kg).

The product distribution at various space times is given in Table 2. As can be seen from Fig. 9, the conversion of 1,4-DIPB increased with an increase in space time; which may be due to the higher contact time between reactants and catalyst. Conversion of 1,4-DIPB was increased to 94.69% at a space time of 9.03 kg h/kmol.

Table 2: Product distribution at various space times.

Product distribution (wt%)	Space Time (kg h/ k mol)					
	4.2	4.8	5.75	7.02	7.9	9.03
Aliphatics	0.71	0.49	0.48	0.04	0.10	0.06
Benzene	68.82	68.25	67.91	62.42	53.97	47.26
Toluene	0.94	0.58	0.29	0.48	0.22	0.35
Xylene	0.32	0.39	0.42	1.03	0.56	1.14
Cumene	16.96	18.78	21.02	28.65	37.39	42.93
n-PB	0.11	0.16	0.23	0.36	0.52	0.57
C10	3.34	2.42	1.14	0.14	0.70	0.96
1,3-DIPB	2.08	4.01	4.29	4.49	4.66	5.16
1,4-DIPB	6.72	4.92	4.22	2.39	1.88	1.57
Cumene yield (%)	16.96	18.78	21.02	28.65	37.39	42.93
1,4-DIPB conv.(wt%)	77.34	83.41	85.77	92.39	93.69	94.69

Reaction Conditions: Pressure =1 atm, temperature = 573 K, benzene/ 1,4-DIPB ratio = 5:1, N_2 to feed ratio = 0.2, time on stream = 30 min, catalyst (CeB_{10}) amount = 0.002 kg.

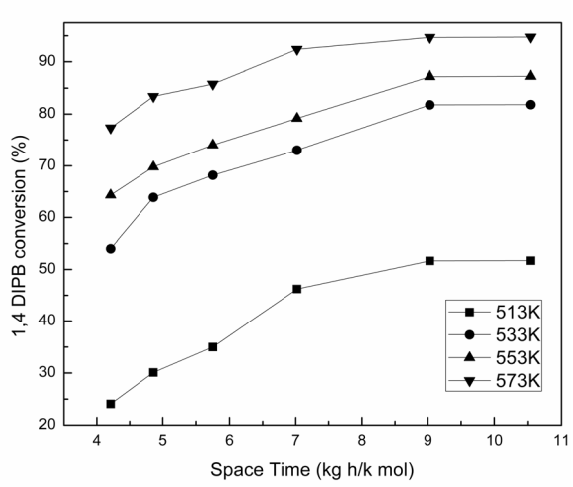

Figure 9: Effect of space time on 1,4-DIPB conversion at different temperatures. Reaction Conditions: Pressure = 1 atm, benzene/1,4-DIPB ratio = 5:1, N_2 to feed ratio = 0.2, time on stream = 30 min, catalyst (CeB_{10}) amount = 0.002 kg.

MASS TRANSFER CONSIDERATIONS

In solid catalyzed gas phase reactions, the effect of external and internal mass transfer resistances may be significant. Experiments were carried out to find the importance of external diffusional resistance by varying feed rates and catalyst size at constant space-time. Table 3 shows that the conversions of 1,4-DIPB at constant space time are independent of feed rate. Therefore, the external mass transfer resistance is negligible. To investigate the effect of intraparticle diffusion the experiments were carried out keeping space-time constant but varying the catalyst particle size. The experimental data shown in Table 4 indicate that the conversion of 1,4-DIPB remain same with catalyst size which indicates negligible intraparticle mass transfer resistance in the particle size range studied.

Table 3: Effect of external diffusional resistances on conversion of 1,4-DIPB over CeB_{10}.

Space-time (kg h/kmol)	Conversion of 1,4-DIPB (%)	
	Catalyst weight = 0.002 kg	Catalyst weight =0.004 kg
4.2	64.34	65.11
4.8	69.80	70.87
5.75	74.03	75.12

Reaction Conditions: Pressure = 1 atm, temperature = 573 K, benzene/ 1,4-DIPB ratio = 5:1, N_2 to feed ratio = 0.2, time on stream = 30 min.

Table 4: Effect of intraparticle diffusional resistance on DIPB conversion over CeB_{10}.

Particle size dp (mm)	Conversion of 1,4-DIPB (%)		
	space-time (kg h/kmol) =4.2	space-time (kg h/kmol) = 4.8	space-time (kg h/kmol) = 5.75
0.50	65.87	70.23	75.34
1.00	65.35	69.98	74.76
1.50	64.34	69.80	74.03

Reaction Conditions: Pressure =1 atm, temperature = 573 K, benzene/ 1,4-DIPB ratio = 5:1, N_2 to feed ratio = 0.2, time on stream = 30 min.

KINETIC MODELLING

The kinetic runs were carried out at four different temperatures. The experiments were conducted in the zone in which mass transfer effects were negligible. Based on the product distribution various kinetic models (adsorption, desorption, and surface reaction control) were formulated following the Langmuir-Hinshelwood approach. These models were tested with the help of the experimental data. A non-linear regression algorithm was used for the kinetic parameter estimation. All models, except one, surface reaction control, were rejected as they resulted in negative kinetic constants. The following rate equation based on surface reaction-control was found to fit the experimental data satisfactorily. Transalkyla-

tion of 1,4 DIPB with benzene is a complex reaction which is followed by isomerization and dispropor-tionation reactions.

i) 1,4-DIPB transalkylation:

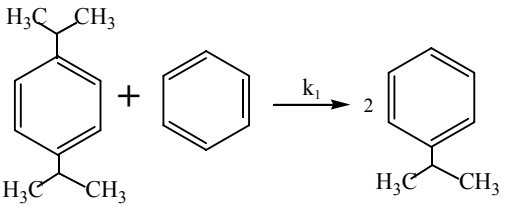

(1)

ii) Isomerisation:

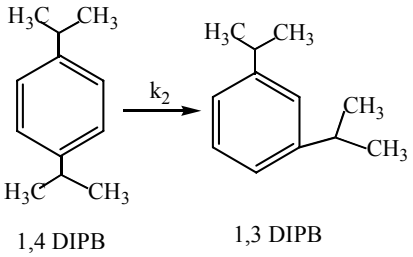

(2)

iii) Dispropotionation:

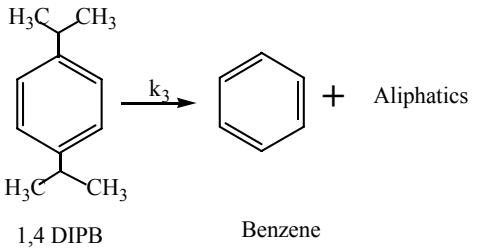

(3)

iv)

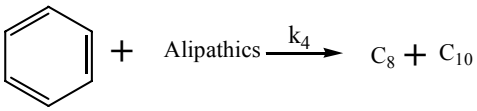

(4)

For the above reactions, the possible rate equations based on different mechanisms are presented below. k_4 is not considered while developing the model because the model is in terms of conversion of 1,4-DIPB and this reaction does not involves DIPB. k_3 is also not considered since only those reactions whose product yield is significant are taken into considerations.

Dual-site mechanism:

$$-r_{DIPB} = C_v^2\left[k_1 k_B\, p_B\, k_{DIPB}\, p_{DIPB} + \left(\frac{k_2}{C_v}\right) k_{DIPB}\, p_{DIPB}\right] \quad (5)$$

where,

$$C_v = \frac{1}{(1 + k_B\, p_B + k_{DIPB}\, p_{DIPB})} \quad (6)$$

Single-site mechanism:

$$-r_{DIPB} = C_v[k_1\, p_B\, k_{DIPB}\, p_{DIPB} + k_2 k_{DIPB}\, p_{DIPB}\,] \quad (7)$$

where,

$$C_v = \frac{1}{(1 + k_B\, p_B)} \quad (8)$$

Stoichiometric model:

$$-r_{DIPB} = [k_1\, p_B\ \ p_{DIPB} + k_2\, p_{DIPB}\,] \quad (9)$$

The partial pressure of 1,4 DIPB and benzene are related to the fractional conversions and the total pressure (P) by these following equations:

$$p_{DIPB} = (1 - X_{DIPB})P / 7.2 \quad (10)$$

$$p_B = (5 - X_B)P / 7.2 \quad (11)$$

$$p_c = (X_c) / 7.2 \quad (12)$$

The optimum values of the parameters were obtained by minimizing the objective function given by the equation:

$$f = \sum\left[(X_{pred})i - (X_{exp})i\right]^2 \quad (13)$$

Model Selection

By using the values of the constants for Equation (5) for the dual site mechanism, as shown in Table 5, the standard error of estimate for the rate of disappearance of 1,4-DIPB was ±3.14 x 10^{-4}. For Equation (6), with the values of the constants from Table 6, the standard error was ± 2.41 x 10^{-3}. For Equation (7), with the values of the constants from Table 7, the standard error was ± 9.92 x 10^{-3}. By comparing the standard errors, model Equation (5) was considered to be the best for representing the reaction system

under investigation. The experimental and the predicted 1,4 DIPB conversions from Equation (5) at four different temperatures are plotted in Fig. 10. The figure shows that the proposed reaction rate expression predicts 1,4-DIPB conversion values quite comparable to the experimental values, having an R^2 value of 0.99. The kinetic constants evaluated and tabulated at various temperatures (Table 5) were used to determine the activation energy for cumene synthesis (transalkylation) which was estimated to be 116.53 kJ/mol; for the isomerisation reaction the activation energy was found to be 176.01 kJ/mol by the following equation:

$$\ln k = \ln A - \frac{E_a}{RT} \tag{14}$$

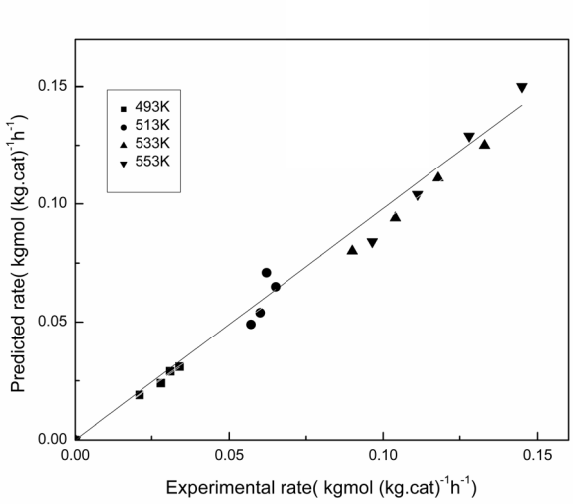

Figure 10: Experimental vs predicted rate of reaction.

Table 5: Kinetic and adsorption constants at different temperature.

Kinetic and adsorption parameters	Temperature (K)			
	493	513	533	553
k_1 (k mol/kg h)	1.11	2.34	10.49	20.53
k_2 (k mol/kg h)	0.097	0.534	4.54	10.54
K_{Dipb} (atm^{-1})	1.223	0.839	0.689	0.459
K_B (atm^{-1})	2.345	2.00	1.80	1.50

The plot of ln k vs 1/T is represented in Fig. 11. The activation energy values for various reactions compare well with the values of similar reactions on zeolites obtained by other investigators (Kondamudi and Upadhyayula, 2008). The kinetic model developed was able to predict the product distribution. Formation of cumene and 1,3-DIPB, the main products, is derived from the equations below.

Rate of formation of cumene:

$$r_c = k_1 k_B \, p_B \;\; k_{DIPB} \, p_{DIPB} \tag{15}$$

Rate of formation of 1,3-DIPB:

$$r_{1,3DIPB} = \left(\frac{k_2}{C_v} \right) k_{DIPB} \, p_{DIPB} \tag{16}$$

k_1, k_2, k_B, k_{DIPB} were estimated by using nonlinear regression analysis using the least square criterion. p_B and p_{DIPB} values can be calculated by the Equations (10) and (11). By using the known parameters k_1, k_2, k_B, k_{DIPB}, p_B, and p_{DIPB}, in Equations (15) and (16), formation of cumene and, in Equation (2), formation of 1,3-DIPB can be predicted.

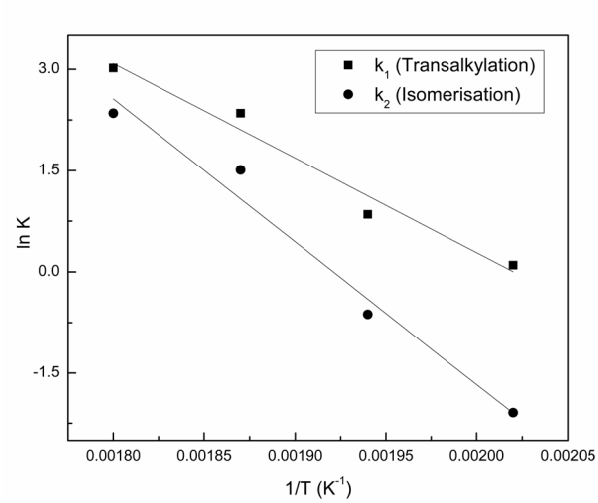

Figure 11: A plot of ln k vs 1/T for determination of the activation energy.

CONCLUSION

The catalytic performance of cerium exchanged beta zeolite was evaluated for the commercially important cumene synthesis. H-beta zeolite was successfully modified with cerium and it was found that activity and selectivity of the cerium-modified zeolite was higher than the parent zeolite due to the presence of strong acid sites in the exchanged zeolite. 94.69% conversion of 1,4-DIPB was obtained over CeB_{10} zeolite with 8.3 wt% Ce content, at 573 K and a benzene to 1,4-DIPB reactant ratio of 5:1. The cumene selectivity in this condition was 83.82%. Based on the product distribution patterns, a kinetic model was proposed and the parameters of the model were estimated. The activation energies for the transalkylation and isomerisation reactions were found to be 116.53 kJ/mol and 176.01 kJ/mol respectively. In industry, using this catalyst, the rate of reaction can be increased, which can save the fixed cost as well as the operating cost by minimizing energy consumption, reactor volume, and reaction time and make the

process more economic. The kinetic model derived for the reactions can provide the necessary information to scale up the reactor for large scale production in industry.

NOMENCLATURE

B	benzene
C	cumene
DIPB	diisopropyl benzene
k_1, k_2, k_3, k_4	kinetic constant (kmol/kg atm^2 h)
K_B	adsorption constant for benzene (atm^{-1})
K_{DIPB}	adsorption constant for DIPB (atm^{-1})
K_C	adsorption constant for cumene (atm^{-1})
P	total pressure (atm)
P_{DIPB}	partial pressure of DIPB (atm)
p_B	partial pressure of benzene (atm)
p_C	partial pressure of cumene (atm)
τ	space-time (kg h/kmol)
X_{DIPB}	fractional conversion of DIPB
X_B	moles of benzene reacted (kmol)
X_C	moles of cumene formed (kmol)
X_{expt}	experimentally measured fractional conversion of DIPB
X_{pred}	model predicted fractional conversion of DIPB

REFERENCES

Amin, N. A. S. and Anggoro, D. D., Characterization and activity of Cr, Cu and Ga Modified ZSM-5 for direct conversion of methane to liquid hydrocarbons. Journal of Natural Gas Chemistry, 12, 123-134 (2003).

Ansari, A. A., Solanki, P. R. and Malhotra, B. D., Hydrogen peroxide sensor based on horse radish peroxidase immobilized nanostructured cerium oxide film. Journal of Biotechnology, 142, 179-184 (2009).

Bakas, S. T. and Barger, P. T., Alkylation/transalkylation process. US Patent 4870222 A (1989).

Barger, P. T., Heights, A., Thompson, G. J. and Herber, R. R., Alkylation/transalkylation process. US patent 4857666(1989).

Barman, S., Pradhan, N. C. and Maity, S. K., Alkylation of toluene with isopropyl alcohol catalyzed by Ce exchanged 13X zeolite catalyst. Journal of Chemical Engineering, 114, 39-45 (2005).

Bellussi, G., Pazzuconi, G., Perego, C., Girotti, G. and Terzoni, G., Liquid phase alkylation of benzene with light olefins catalyzed by beta zeolite. Journal of Catalysis, 157, 227-231 (1995).

Best, D. A. and Wojciechowski, B. W., The kinetics of the catalytic isomerization and transalkylation of cumene. Journal of Catalysis, 53, 243-250 (1978).

Collins, N. A., Mazzone, D. N. and Venkat C. R., Alkylaromatics production. US Patent 5902917 A (1999).

Ercan, C., Dautzenberg, F. M., Yeh, C. Y. and Barner, H. E., Mass-transfer effects in liquid-phase alkylation of benzene with zeolite catalysts. Industrial Engineering Chemistry Research, 37, 1724-1728 (1998).

Kiricsi, I., Flego, C., Pazzuconi, G., Parker, W. O. Jr., Millini, R., Perego, C. and Bellussi, G., Progress toward understanding zeolite beta acidity: An IR and 27Al NMR spectroscopic study. Journal of Physical Chemistry, 98, 4627-4634 (1994).

Garcia, F. A. C., Araujo, D. R., Silva, J. C. M., Macedo, J. L., Ghesti, G. F., Dias, S. C. L., Diasa, J. A. and Geraldo, N. R., Effect of cerium loading on structure and morphology of modified Ce-USY zeolites. Journal of Brazilian Chemical Society, 22, 1894-1902 (2011).

Grigore, B., Mihai, L., Elena, Z. and Raluca, M., Kinetics of diisopropylbenzene transalkylation with benzene on a Ca modified YH zeolite catalyst. Proceedings Romanian International Conference on Chemistry and Chemical Engineering (2001).

Halgeri, A. B. and Das, J., Novel catalytic aspects of beta zeolite for alkyl aromatics transformation. Applied Catalysis, A, 181, 347-354 (1999).

Huang, Z., Tian, S., Xu, Y., Zhu, B. and Wang, W., Zeolite catalyst for the liquid phase alkylation and transalkylation of benzene. US patent 5600050 (1997).

Hunter, F. D. and Scherzer, J., Cation positions in cerium X zeolites. Journal of Catalysis, 20, 246-259 (1971).

Kondamudi, K. and Upadhyayula, S., Transalkylation of diisopropylbenzene with benzene over SAPO-5 catalyst: A kinetic study. Journal of Chemical Technology and Biotechnology, 83, 699-706 (2008).

Krishnan, A. V., Ojha, K., and Pradhan, N. C., Alkylation of phenol with tertiary butyl alcohol over zeolites. Organic Process Research and Development, 6, 132-137 (2002).

Leu, L. J., Kang, B. C., Wu, S. T. and Wu, J. C., Toluene disproportionation reaction over modified HY and LaHY catalysts. Applied Catalysis, A, 63, 91-106 (1990).

Maity, S. and Pradhan, N. C., Kinetics of transalkyla-

tion of diisopropylbenzene with benzene, Proceedings CHEMCON, Ankleswar, Gujrat (2006).

Perego, C. and Ingallina, P., Combining alkylation and transalkylation for alkylaromatic production. Green Chemistry, 6, 274-279 (2004).

Perego, C., Amarilli, S., Millini, R., Bellussi, G., Girotti, G. and Terzoni, G., Experimental and computational study of beta, ZSM-12, Y, mordenite and ERB-1 in cumene synthesis. Microporous Material, 6, 395-404 (1996).

Pradhan, A. R. and Rao, B. S, Transalkylation of diiopropylbenzenes over large pore zeolites. Applied Catalysis, A, 106, 143-153 (1993).

Rabo, J. A., Angell, C. L. and Schomaker, V., Catalytic and structural properties of rare-earth exchanged forms of type Y zeolite. Proc. 4th Intl. Congr. Catal., (Moscow), 96 (1968).

Reddy, K. S. N., Rao, B. S. and Shiralkar, V. P., Alkylation of benzene with isopropanol with zeolite beta. Applied Catalysis, A, 95, 53-63 (1993).

Slaugh, L. H., Process for transalkylating benzene and dialkybenzene. US Patent 4375574 A (1983).

Siregar, T. B. and Amin, N. A. S., Catalytic cracking of palm oil to gasoline over pretreated Cu-ZSM-5. Jurnal Teknologi, 44, 69-82 (2006).

Smirnov, A. V., Renzo, D. F., Lebedeva, O. E., Brunel, D., Chiche, B., Tavolaro, A., Romanovsky, B. V., Giordano, G., Fajula, F. and Ivanova, I. I., Selective benezene isopropylation over Fe-containing zeolite beta. Studies in Surface Science and Catalysis, 105, 1325-1332 (1997).

Sotelo, J. L., Calvo, L., Perez-Velazquez, A., Cavani, F. and Bolognini, M., A comparative study on the transalkylation of diisopropylbenzene with benzene over several zeolitic materials in supercritical CO_2 and liquid phase. Applied Catalysis, A, 312, 194-201 (2006).

Sridevi, U., Rao, B. K. B., Pradhan, N. C., Tambe, S. S., Satyanarayana, C. V. and Rao, B. S., Kinetics of isopropylation of benzene over H-beta catalyst. Industrial Engineering Chemistry Research, 40, 3133-3138 (2001).

Tang, B., Dai, W., Sun, X., Guan, N., Li, L. and Hunger, M., A procedure for the preparation of Ti-Beta zeolitesfor catalytic epoxidation with hydrogen peroxide. Green Chemistry, 16, 2281-2291 (2014).

Thakur, R., Barman, S. and Gupta, R., Synthesis of xylene over cerium modified large pore zeolite. Indian Journal of Chemical Technology, 21, 379-385 (2014).

Thakur, R., Gupta, R. and Barman, S., Optimization of process parameters for transalkylation of toluene to xylene using response surface methodology. Particulate Science and Technology: An International Journal, Accepted Article, (DOI: 10.1080/02726351.2015.1081656).

Venuto, P. B., Hamilton, L. A., Landis, P. S. and Wise, J. J., Organic reactions catalyzed by crystalline aluminosilicates: I. Alkylation reactions. Journal of Catalysis, 5, 81-98 (1966).

Wang, H. and Zou, Y., Modified beta zeolite as catalyst for fries rearrangement reaction. Catalysis Letters, 86, 163-167 (2003).

Yeh, C. Y., Xu, J., Hillsborough, N. J., Angevine, P. J. and Woodbury, N. J., Process for benzene alkylation and transalkylation of polyalkylated aromatics over improved zeolite beta catalyst. US patent 737190B2 (2008).

Zhang, Q., Ming, W., Ma, J., Zhang, J., Wang, P. and Li, R., De novo assembly of a mesoporous beta zeolite with intracrystalline channels and its catalytic performance for biodiesel production. Journal of Materials Chemistry, A, 2, 8712-8718 (2014).